AP

The Enzymatic Formation of Novel Bile Acid Primary Amides

Lawrence King III,* Stephen Barnes,† Uta Glufke,‡ Matthias E. Henz,‡ Marion Kirk,†
Kathleen A. Merkler,*,§ John C. Vederas,‡ Benjamin J. Wilcox,* and David J. Merkler*,§[,1]

*Department of Chemistry and Biochemistry, Duquesne University, Pittsburgh, Pennsylvania 15282; †Department of Pharmacology and Toxicology and Comprehensive Cancer Center Mass Spectrometry Shared Facility, University of Alabama at Birmingham, Birmingham, Alabama 35294; ‡Department of Chemistry, University of Alberta, Edmonton, Alberta, Canada T6G 2G2; and §Department of Chemistry, University of South Florida, Tampa, Florida 33620

Bifunctional peptidylglycine α-amidating monooxygenase (PAM) catalyzes the copper-, ascorbate-, and O_2-dependent cleavage of C-terminal glycine-extended peptides and N-acylglycines to the corresponding amides and glyoxylate. The α-amidated peptides and the long-chain acylamides are hormones in humans and other mammals. Bile acid glycine conjugates are also substrates for PAM leading to the formation of bile acid amides. The $(V_{MAX}/K_m)_{app}$ values for the bile acid glycine conjugates are comparable to other known PAM substrates. The highest $(V_{MAX}/K_m)_{app}$ value, $3.1 \pm 0.12 \times 10^5 \ M^{-1} \ s^{-1}$ for 3-sulfolithocholylglycine, is 6.7-fold higher than that for D-Tyr–Val–Gly, a representative peptide substrate. The time course for O_2 consumption and glyoxylate production indicates that bile acid glycine conjugate amidation is a two-step reaction. The bile acid glycine conjugate is first converted to an N-bile acyl-α-hydroxyglycine intermediate which is ultimately dealkylated to the bile acid amide and glyoxylate. The enzymatically produced bile acid amides and the carbinolamide intermediates were characterized by mass spectrometry and two-dimensional $^1H–^{13}C$ heteronuclear multiple quantum coherence NMR.   © 2000 Academic Press

Key Words: peptidylglycine α-amidating monooxygenase; bile acid glycine conjugate; cholylglycine; carbinolamide intermediate.

Two classes of amidated hormones are known from living systems. A majority of the peptide hormones in mammals (1), insects (2), and cnidarians (3) have a C-terminal α-amide moiety and fatty acid primary amides like oleamide (4) and erucamide (5) are now recognized as cell signaling molecules in humans and other mammals. Structure–activity studies indicate that the amide moiety is critical to the bioactivity of the amidated peptide hormones (1) and the fatty acid primary amides (6). Peptidylglycine α-amidating monooxygenase (PAM, EC 1.14.17.3)[2] has a well-established

[2] Abbreviations used: Ac, acetyl; ACGNAT, acyl-CoA:glycine N-acyltransferase; dansyl, 5-(dimethylamino)napthalene-1-sulfonyl; ESI, electrospray ionization; Hepes, 4-(2-hydroxyethyl)-1-piperazineethanesulfonic acid; HMQC, heteronuclear multiple quantum coherence; HPLC, high-performance liquid chromatography; LC, liquid chromatography; Mes, 2-(*N*-morpholino)ethane sulfonic acid; MS, mass spectrometry; MS-MS, tandem mass spectrometry; PAL, monofunctional peptidylamidoglycolate lyase; PAM, bifunctional peptidylglycine α-amidating monooxygenase; and PHM, monofunctional peptidyl α-hydroxylating monooxygenase.

role in the biosynthesis of α-amidated peptide hormones (7–9) and has been proposed to be involved in the biosynthesis of the fatty acid primary amides (10).

PAM is a bifunctional, copper- and zinc-dependent monooxygenase that catalyzes the oxidative cleavage of C-terminal glycine-extended peptide precursors and N-fatty acylglycines to the corresponding amidated hormones and glyoxylate (for recent reviews, see Refs. 11, 12). Recently, we have reported that the $(V_{MAX}/K_m)_{app}$ for N-acylglycine amidation increases as the length of the acyl chain increases, reaching a plateau value that is comparable to that obtained with the glycine-extended peptide substrates (13). For example, the $(V_{MAX}/K_m)_{app}$ for N-decanoylglycine amidation is 3.3-fold higher than the value obtained for D-Tyr–Val–Gly, a representative peptide substrate. The N-acyl-glycines are produced enzymatically from the acyl-CoA thioesters and glycine by acyl-CoA:glycine N-acyl-transferase (ACGNAT, EC 2.3.1.13) (14, 15). ACGNAT is found primarily in the liver and kidney, but does colocalize with PAM in the cerebrum and the cerebellum (16, 17). The discovery that PAM efficiently amidates N-fatty acylglycines (10, 13) suggests that the enzyme may have role in the biosynthesis of fatty acid primary amides in vivo and is a lead for the development of novel therapeutics specifically targeted against PAM. In addition, PAM may also amidate other biologically occurring, nonpeptide substrates leading to the formation of other undiscovered carboxamidated compounds.

One possible class of unrecognized, nonpeptide substrates for PAM that occurs physiologically is the bile acid glycine conjugates. These compounds are made in the liver (20), a tissue that does not contain PAM activity (17–19). However, liver disease can result in a substantial elevation (~50 μM) in bile acid glycine conjugates in serum (21, 22) and PAM is found in serum (17, 18). The circulating bile acid glycine conjugates might also be transported to tissues that contain high levels of PAM like the hypothalamus, the pituitary, or the atrium (17, 18, 23).

We now report that PAM will amidate the bile acid glycine conjugates to the bile acid amides. These compounds, whose structures diverge considerably from those of the glycine-extended peptides and the N-acyl-glycines, are excellent substrates with $(V_{MAX}/K_m)_{app}$ values that are two- to sevenfold higher than that measured for D-Tyr–Val–Gly. We further show that N-cholyl-α-hydroxyglycine is an intermediate in the PAM-catalyzed amidation of cholylglycine to cholana-mide.

EXPERIMENTAL PROCEDURES

Materials. Sodium salts of chenodeoxycholylglycine, deoxycholyl-glycine, 3-sulfolithocholylglycine and cholyltaurine, N-dansyl-Tyr–

Val–Gly, D-Tyr–Val–Gly, sodium ascorbate, rabbit muscle lactate dehydrogenase, glyoxylic acid monohydrate, and NADH were obtained from Sigma Chemical Co. (St. Louis, MO), N-acetylglycine and [glycyl-1,2-$^{13}C_2$]cholylglycine was obtained from Aldrich Chemical Co. (Milwaukee, WI), and the sodium salt of cholylglycine was from Fluka Biochemicals (Milwaukee, WI). N-Acetyl-L-phenylala-nylpyruvate (N-Ac-Phe-pyruvate, 2,4-diketo-5-acetamido-6-phenyl-hexanoic acid) was synthesized as described (24), but with a modified hydrolysis procedure (13). All other reagents were of the highest quality available commercially.

Initial rate studies. Reactions at 37.0 ± 0.1°C were initiated by the addition of PAM (10–50 μg) into 2.4 ml of 100 mM Mes/NaOH, pH 6.0, 30 mM NaCl, 1% (v/v) ethanol, 0.001% (v/v) Triton X-100, 1.0 μM Cu(NO$_3$)$_2$, 5.0 mM sodium ascorbate, and the bile acid glycine conjugate (generally 0.2 $K_{m,app}$ to 3.0 $K_{m,app}$). Initial rates were measured by following the PAM-dependent consumption of O$_2$ using a Yellow Springs Instrument Model 53 oxygen monitor. $V_{MAX,app}$ values were normalized to controls performed at 11.0 mM N-acetylglycine. Ethanol was added to protect the catalase against ascorbate-mediated inactivation and Triton X-100 was included to prevent nonspecific absorption of the enzyme to the sides of the oxygen monitor chambers.

Bifunctional peptidylglycine α-amidating monooxygenase. Chinese hamster ovary cells that secrete recombinant type A rat medullary thyroid carcinoma PAM into the culture media (25) were grown in a Cellco Cellmax-100 hollow fiber bioreactor (26). The bifunctional enzyme was purified as described by Miller et al. (27) except that the final gel filtration step (Sephacryl S-300) was done using 20 mM Hepes/NaOH, pH 7.8, 50 mM NaCl, 0.001% (v/v) Triton X-100. The amidation of N-dansyl-Tyr–Val–Gly to N-dansyl-Tyr–Val–NH$_2$ (28) was used throughout the enzyme purification to screen column fractions. Unless noted, the PAM used in these studies had a specific activity of ≥3.0 μmol of O$_2$ consumed/min/mg at 37°C under standard conditions. Standard conditions were as follows: 100 mM Mes/NaOH, pH 6.0, 30 mM NaCl, 1% (v/v) ethanol, 0.001% (v/v) Triton X-100, 10 μg/ml bovine catalase, 1.0 μM Cu(NO$_3$)$_2$, 5.0 mM sodium ascorbate, and 11.0 mM N-acetylglycine.

Glyoxylate determination. Glyoxylate was determined by the spectrophotometric method of Christman et al. (29) as modified by Katopodis and May (30). Standard curves of [glyoxylate] vs A_{520} were constructed in the appropriate buffers using a glyoxylate solution that had been calibrated by measuring the glyoxylate-dependent oxidation of NADH ($\Delta\epsilon_{340} = 6.22 \times 10^3$ M^{-1} cm^{-1}) as catalyzed by lactate dehydrogenase.

HMQC NMR analysis of the PAM conversion of [glycyl-1,2-$^{13}C_2$]cholylglycine. Experiment A: The solution contained 3.0 mM [glycyl-1,2-$^{13}C_2$]-cholylglycine, 10 μg/mL bovine catalase, 1.0 μM Cu(NO$_3$)$_2$, 4.0 mM sodium ascorbate, 100 μM N-Ac-Phe-pyruvate, 150 μg/mL PAM in 10 mM Mes/LiOD, pD 5.6, 4.0 mM NaCl (D$_2$O), total reaction volume = 1.6 mL. Sodium ascorbate, N-Ac-Phe-pyru-vate, and NaCl were diluted from concentrated stocks prepared in D$_2$O such that the final reaction mixtures contained 88% (v/v) D$_2$O. The reaction mixture was incubated at 37°C for 3 h, after which time PAM was removed by ultrafiltration using an Amicon Centricon-30 filter. Experiment B: The reaction was done in a manner analogous to that of experiment A, but no PAM and no N-Ac-Phe-pyruvate were added to provide a control. Experiment C: The reaction was done in a manner analogous to that of experiment A, but no N-Ac-Phe-pyruvate was added.

An aliquot (0.7 mL) of each of the reaction mixtures (A, B, and C) was taken and analyzed by HMQC NMR using an Inova 600 Varian instrument (parameters: temperature, 27°C; solvent, D$_2$O; number of transients, 32; number of increments, 256; number of data points, 6464; acquisition time, 0.8 s; sweep width, 15087 Hz in F1 (^{13}C chemical shift) and 4002 Hz in F2 (^1H chemical shift)). Solvent

presaturation was used for 1.2 s, and no ^{1}H, ^{13}C decoupling was applied. The HMQC NMR of sample A shows the doublets for [*glycyl*-1,2-^{13}C$_2$]cholylglycine (F1, 44.0 ppm; F2, 3.76 ppm; J_{CH}, 138 Hz), for the corresponding [*glycyl*-1,2-^{13}C$_2$]-*N*-cholyl-α-hydroxyglycine (F1, 73.4 ppm; F2, 5.33 ppm; J_{CH}, 154 Hz), and for the hydrate of [1,2-^{13}C$_2$]glyoxylate (F1, 89.0 ppm; F2, 5.06 ppm; J_{CH}, 165 Hz). The chemical shifts were referenced to 1% external acetone. The HMQC NMR of sample B shows only the doublet for the starting material. The HMQC NMR of sample C shows the doublets for the starting material and the hydrate of [1,2-^{13}C$_2$]glyoxylate.

LC-MS. Aliquots of reaction mixtures were analyzed by reversed-phase HPLC, using a 2.1-mm-i.d. × 15-cm Brownlee Aquapore C$_8$ 5-μm column. The mobile phase was a linear 30–100% gradient of acetonitrile in 0.1% (v/v) aqueous formic acid at a flow rate of 0.2 ml/min. The eluent was split 1:1 with 0.1 ml/min passed into the IonSpray interface of a PE-Sciex (Concorde, Ontario, Canada) API III triple quadrupole mass spectrometer. For positive ion spectra, the IonSpray needle voltage and the orifice potential were set at +5400 and 60–75 V, respectively. The corresponding voltages for negative ion spectra were −4900 and −60 to −70 V. Mass spectra were collected over a m/z range of 300–600. To collect MS-MS data, parent molecular ions were selected in the first quadrupole, collided with 90% Ar–10% N$_2$, and the resulting daughter ions analyzed in the third quadrupole. Data were processed using software provided by the manufacturer.

Data analysis. Kinetic parameters for linear double reciprocal plots were fit to

$$v = (V_{MAX,app}[A])/(K_{m,app} + [A]), \qquad [1]$$

where $K_{m,app}$ is the apparent Michaelis constant for the bile acid glycine conjugate, A, at constant fixed concentrations of ascorbate and O$_2$, and $V_{MAX,app}$ is the apparent catalytic rate at saturating $[A]$ under the conditions of the experiment (31).

RESULTS

Steady-state kinetic studies. Addition of PAM to cholylglycine, deoxycholylglycine, chenodeoxycholylglycine, or 3-sulfolithocholylglycine results in the consumption of O$_2$. The initial rate of O$_2$ consumption increases as the initial concentration of the bile acid glycine conjugate increases. Analysis of the substrate concentration dependence of the initial rates generates the steady-state kinetic parameters summarized in Table I. The highest $(V_{MAX}/K_m)_{app}$ value obtained for the oxidation of a bile acid glycine conjugate was 3-sulfolithocholylglycine, $3.1 \pm 0.12 \times 10^5 \, M^{-1} \, s^{-1}$. This value is 6.7-fold higher than the value obtained for the oxidation of D-Tyr–Val–Gly and is comparable to the best glycine-extended peptide (32)[3] and the *N*-acylglycine
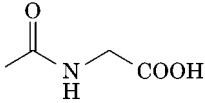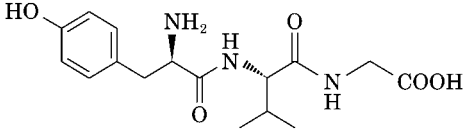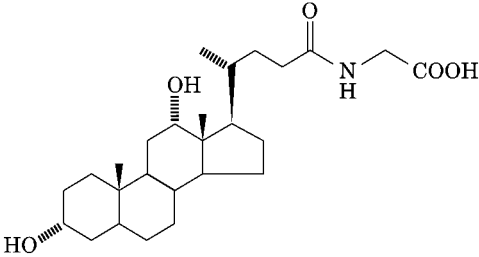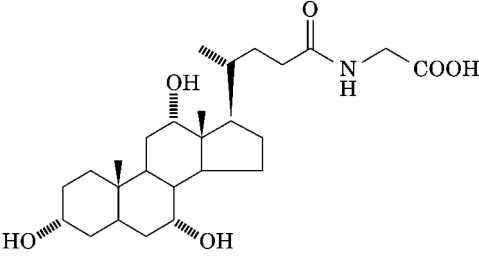
---

[3] Tamburini *et al.* (32) determined the kinetic parameters for the PAM-catalyzed oxidation of a set of glycine-extended peptides of the form *N*-dansyl-(Gly)$_4$–*X*–Gly in which the amino acid at position *X* was substituted with each of the 20 amino acids commonly found in proteins. Because of experimental differences, these data are difficult to directly compare to the data presented here. However, the $(V_{MAX}/K_m)_{app}$ for the best substrate, *N*-dansyl-(Gly)$_4$–Phe–Gly, was 12.8-fold higher than the $(V_{MAX}/K_m)_{app}$ for *N*-dansyl-(Gly)$_4$–Val–Gly.
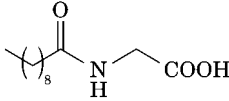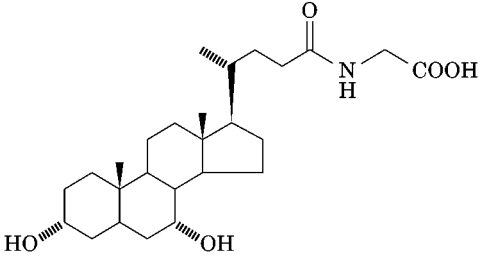
substrates (13). For example, the ratio of the $(V_{MAX}/K_m)_{glycolithocholate-3-sulfate}/(V_{MAX}/K_m)_{acetylglycine}$ is 370 while the ratio of $(V_{MAX}/K_m)_{oleoylglycine}/(V_{MAX}/K_m)_{acetylglycine}$ is 380. Cholyltaurine is neither a substrate nor an inhibitor for PAM, consistent with substrate specificity studies showing that only glycine-extended and D-alanine-extended peptides are amidated by bifunctional PAM (33).

Oxidation of the bile acid glycine conjugates. The data in Table I are evidence only for the PAM-dependent oxidation of O$_2$ in the presence of the bile acid glycine conjugates and ascorbate. Uncoupling of substrate oxidation from ascorbate oxidation by the bile acid glycine conjugates would result in the O$_2$ consumption with little formation of the bile acid amides and glyoxylate. Conclusive proof for the oxidation of the bile acid glycine conjugates requires the identification of the reaction products (see below). The PAM-dependent formation of glyoxylate from the bile acid glycine conjugates provides a convenient, general assay for the cleavage of the C$_\alpha$–N bond in the glycine moiety. Glyoxylate production upon the amidation of the glycine-extended peptides (7, 34), the *N*-acylglycines (13), and hippurate (*N*-benzoylglycine) (30) has been reported. Incubation of the bile acid glycine conjugates with PAM and ascorbate leads to the formation of glyoxylate (Table II). The PAM-dependent consumption of O$_2$ shown in Table I does lead to the oxidative cleavage of the bile acid glycine conjugates.

Isolation and characterization of the enzymatically produced bile acid amides. Analysis of the reaction mixture with cholylglycine as the substrate by LC-MS in the positive ion mode shows the disappearance of the m/z 466 $[M + H]^+$ cholylglycine molecular ion and the appearance of a m/z 408 $[M + H]^+$ molecular ion for cholanamide (Figs. 1A and 1B). The second peak in Fig. 1B is due to the ammonia adduct $[M + 17]^+$ of an ion of m/z of 391, believed to be a detergent. The positive daughter ion spectrum of the cholanamide molecular ion (m/z 408) contained major fragments at m/z 372 $[M - (2 \times H_2O)]^+$, m/z 354 $[M - (3 \times H_2O)]^+$, m/z 337 $[M–A\text{-ring}]^+$, and m/z 319 $[M - (A\text{-ring} + H_2O)]^+$ (Fig. 2). In the negative ion mode, the m/z 464 $[M - H]^-$ cholylglycine molecular ion disappeared and a m/z 466 $[M + 60 - H]^-$ cholanamide–acetate adduct molecular ion appeared (data not shown). A similar pattern of results was obtained upon the analysis of the reaction products generated by incubating PAM with deoxycholylglycine and chenodeoxycholylglycine. The m/z values as determined by LC-MS for the products of the reaction of PAM with cholylglycine, deoxycholylglycine, chenodeoxycholylglycine, and 3-sulfolithocholylglycine are summarized in Table III.
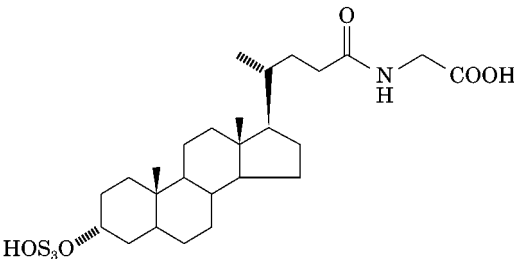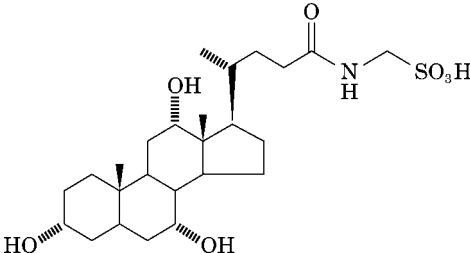
TABLE I

Kinetic Constants for Bile Acid Glycine Conjugate Amidation

Substrate	Structure	$K_{m,app}$ (μM)	$V_{MAX,app}$ (μmol/min/mg)	$(V_{MAX}/K_m)_{app}$ (M^{-1} s^{-1})	Relative $(V_{MAX}/K_m)_{app}$
N-Acetylglycine[a]		9300 ± 470	6.4 ± 0.15	860 ± 30	0.018
D-Tyr–Val–Gly		220 ± 31	7.9 ± 0.78	$(4.6 \pm 0.22) \times 10^4$	1.0
Deoxycholylglycine (glycodeoxycholate)		150 ± 12	12 ± 0.49	$(1.0 \pm 0.039) \times 10^5$	2.2
Cholylglycine (glycocholate)		94 ± 8.0	8.5 ± 0.26	$(1.1 \pm 0.072) \times 10^5$	2.4
N-Decanoylglycine[a]		100 ± 4.1	13 ± 0.19	$(1.1 \pm 0.072) \times 10^5$	3.3
Chenodeoxycholylglycine (glycochenodeoxycholate)		56 ± 4.0	8.5 ± 0.25	$(1.9 \pm 0.082) \times 10^5$	4.1

Amidation of the bile acid glycine conjugates proceeds via a carbinolamide intermediate. The amidation of the glycine-extended peptides (35, 36) and the N-acylglycines (13) occurs in two steps. In the first step, O$_2$-dependent hydroxylation of the glycyl α-carbon forms a carbinolamide (36). In the second step, O$_2$-independent dealkylation of the carbinolamide yields the amide and glyoxylate (37). Each step is catalyzed by a separate catalytic domain in bifunctional PAM. Peptidyl α-hydroxylating monooxygenase (PHM) catalyzes the hydroxylation reaction and peptidylamidoglycolate lyase (PAL) catalyzes the dealkylation re-

TABLE I—*Continued*

Substrate	Structure	$K_{m,\text{app}}$ (μM)	$V_{\text{MAX,app}}$ (μmol/min/mg)	$(V_{\text{MAX}}/K_m)_{\text{app}}$ (M^{-1} s^{-1})	Relative $(V_{\text{MAX}}/K_m)_{\text{app}}$
3-Sulfolithocholylglycine (glycolithocholate-3-sulfate)		46 ± 3.4	12 ± 0.43	$(3.1 \pm 0.012) \times 10^5$	6.7
Cholyltaurine[b] (taurocholate)		—	0	—	—

Note. Reactions were carried out at 37°C in 100 mM Mes/NaOH pH 6.0, 30 mM NaCl, 1.0% (v/v) ethanol, 0.001% (v/v) Triton X-100, 5.0 mM sodium ascorbate, 1.0 μM Cu(NO$_3$)$_2$, 10 μg/ml catalase, and the indicated bile acid glycine conjugate. Initial rates were measured by following the PAM-dependent consumption of O$_2$. Kinetic constants $\pm$ standard error are from computer fits of the initial rate data to the Michaelis–Menton equation.

[a] Data taken from Wilcox *et al.* (13). These data are included to provide a comparison between the kinetic constants for *N*-acylglycine amidation and bile acid glycine conjugate amidation. Longer chain *N*-acylglycines like *N*-myristoylglycine and *N*-oleoylglycine have $(V_{\text{MAX}}/K_m)_{\text{app}}$ values ~2-fold higher than *N*-decanoylglycine, but are difficult to compare directly because DMSO was included in the reaction solutions to overcome solubility problems.

[b] No O$_2$ consumption was found upon the addition of PAM to 50 μM, 200 μM, or 520 μM cholyltaurine. In addition, 10–160 μM cholyltaurine did not inhibit the PAM-catalyzed consumption of O$_2$ at 5.0 mM *N*-acetylglycine.

action. The presence of an alternatively spliced dibasic amino acid processing site between the PHM and PAL domains in bifunctional PAM facilitates the proteolytic separation of PHM and PAL into individual catalytic units (25, 38).

The addition of PAM to 75 μM cholylglycine results in the consumption of O$_2$ and the production of glyoxylate (Fig. 3). However, the rate of glyoxylate production is ~4-fold slower than the rate of O$_2$ consumption. This result indicates that there must be the initial formation of an oxidized intermediate from cholylglycine which then decays to the glyoxylate. A second reaction done in the presence of 22.5 μM *N*-Ac-Phe-pyruvate, a PAL-specific inhibitor with a $K_i = 0.24$ μM (24), shows >50-fold decrease in the rate of glyoxylate production with almost no effect on the rate of O$_2$ consumption (Fig. 3). The accumulation of sufficient amounts of the oxidized intermediate for chemical analysis can be accomplished by performing the reaction in the presence of *N*-Ac-Phe-pyruvate.

The oxidized intermediate formed from cholylglycine is likely to be a carbinolamide, *N*-cholyl-α-hydroxygly-cine (Scheme I). The ^{13}C chemical shift of the glycyl α-carbon will be ~45 ppm in cholylglycine, ~75 ppm in *N*-cholyl-α-hydroxyglycine, and ~90 ppm in glyoxylate (39). The ^{13}C chemical shift of the glycyl α-carbon is, thus, diagnostic of carbinolamide formation. Incubation of [*glycyl*-1,2-^{13}C]cholylglycine with PAM in the presence of *N*-Ac-Phe-pyruvate results in a downfield shift in ^{13}C chemical shift of the glycyl α-carbon from 44.0 ppm (Fig. 4A) to 73.4 ppm (Fig. 4B), consistent with the formation of *N*-cholyl-α-hydroxyglycine. LC-MS analysis of a similar reaction done using unlabeled cholylglycine reveals two species, one the acetate adduct of cholanamide (*m/z* 466 [*M* + 60 − H]$^-$ (Fig. 5A) and the other at *m/z* 480 (Fig. 5B), the [*M* − H]$^-$ molecular ion of *N*-cholyl-α-hydroxyglycine (C$_{26}$H$_{43}$NO$_7$ = 481.6 Da). MS-MS spectra of the *m/z* 480 ion contained a major *m/z* 73 fragment ion representing cleavage of the hydroxyglycine moiety (data not shown). A minor fragment ion at *m/z* 462 resulted from loss of water from the molecular [*M* − H]$^-$ ion, presumably from the hydroxyglycine group. The NMR and LC-MS data show that the oxidized intermediate initially formed from cholylglycine

The PAM-Dependent Formation of Glyoxylate from the Bile Acid Glycine Conjugates

Substrate	Glyoxylate Produced (μM)
Chenodeoxycholylglycine	94 ± 5
Cholylglycine	103 ± 12
Deoxycholylglycine	112 ± 12
3-Sulfolithocholylglycine	130 ± 13

Note. Reactions were initiated by the addition of 17 μg of PAM into 1.2 ml of 100 mM Mes/NaOH, pH 6.0, 30 mM NaCl, 1.0% (v/v) ethanol, 0.001% (v/v) Triton X-100, 5.0 mM sodium ascorbate, 1.0 μM Cu(NO$_3$)$_2$, 10 μg/ml catalase, and 150 μM bile acid glycine conjugate. After 3 h at 37°C, reactions were terminated by the addition of 200 μl of 6% (v/v) trifluoroacetic acid and glyoxylate was determined spectrophotometrically (see Experimental Procedures). No glyoxylate was formed in controls lacking the glycine conjugate or PAM. Error bars represent the standard deviation of duplicate reactions.

is the carbinolamide, *N*-cholyl-α-hydroxyglycine. Incubations of PAM with deoxycholylglycine and chenodeoxycholylglycine done in the presence of the PAL-specific inhibitor also show evidence for the formation of the carbinolamide intermediate (Table III).

DISCUSSION

Bile acid glycine conjugates as PAM substrates. PAM preferentially amidates C-terminal glycine-extended peptides with a penultimate hydrophobic amino acid (32). In addition, Erion *et al.* (40) have shown that the affinity of PAM for C-terminal homocysteine-extended peptide inhibitors increases when the penultimate residue is a hydrophobic amino acid. The bile acid glycine conjugates possess a hydrophobic steroid moiety adjacent to the glycyl residue and prove to be excellent substrates for PAM. The (V_{MAX}/K_m)$_{app}$ values for all the bile acid glycine conjugates tested in this study are greater than the (V_{MAX}/K_m)$_{app}$ value measured for a representative peptide substrate, D-Tyr–Val–Gly, and compare favorably with (V_{MAX}/K_m)$_{app}$ values measured for the best long-chain *N*-acylglycine (13) and C-terminal glycine-extended peptide substrates (32) (Table I).[3]

PHM is a prolate ellipsoid composed of two separate domains that form a highly hydrophobic pocket (41). It may be that the steroid moiety of the bile acid glycine conjugates intercalates between these domains and thereby positions the glycyl moiety in the active site. The approximately threefold variation in the (V_{MAX}/K_m)$_{app}$ for the bile acid glycine conjugates may result from differences in their binding to PHM as consequence of the decoration of the steroid moiety with a differing ensemble of hydroxyl or sulfate functionalities. The cocrystallization of PAM with a bile acid

glycine conjugate would provide considerable information concerning the interactions of the enzyme with this class of nonpeptide substrates.

Characterization of the enzymatically generated reaction products. The kinetic constants shown in Table I were generated by measuring the PAM-dependent consumption of O$_2$ in the presence of the bile acid glycine conjugate and ascorbate. These data are not proof of the oxidative modification/cleavage of the bile acid glycine conjugate, but instead could represent the
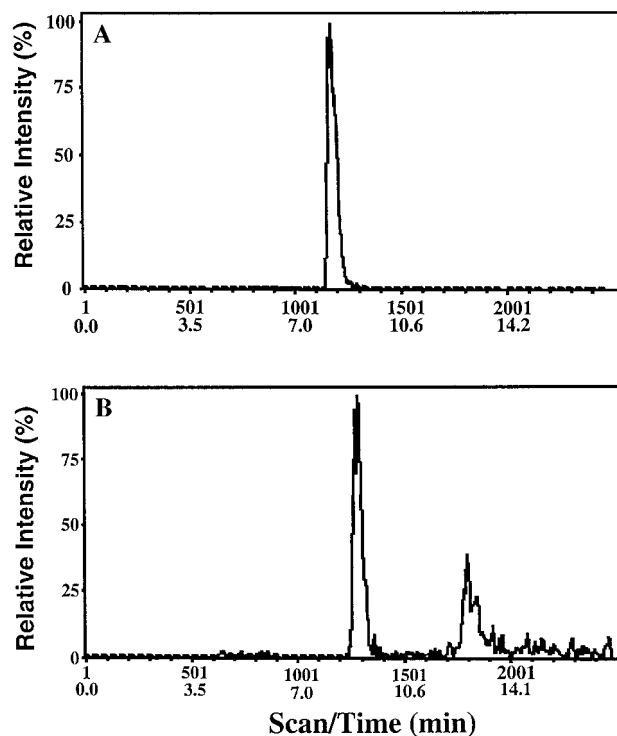

FIG. 1. LC-ESI-MS selected ion chromatogram of the reaction of cholylglycine with PAM. Reactions at 37°C were initiated by the addition of PAM (37 μg) to 3.5 ml of 20 mM Mes/NaOH, pH 6.0, 0.001% (v/v) Triton X-100, 10 μg/ml catalase, 1.0 μM Cu(NO$_3$)$_2$, 1.0 mM sodium ascorbate, and 200 μM cholylglycine. The reaction was allowed to continue until O$_2$ consumption had ceased (12 min) and the sample was frozen immediately with liquid N$_2$. Aliquots (5 μl) of the incubation mixture were analyzed by reversed-phase HPLC, using a 2.1-mm-i.d. × 15-cm Brownlee Aquapore C$_8$ 5 μm column and a mobile phase of a linear 30–100% gradient of acetonitrile in 0.1% aqueous acetic acid at a flow rate of 0.2 ml/min. The eluent was split 1:1 with 0.1 ml/min passed into the IonSpray interface of a PE-Sciex API III triple quadrupole mass spectrometer. The IonSpray needle voltage was +5400 V and the orifice potential +60 V. Mass spectra were collected over a *m/z* range of 300–600. The chromatograms in A and B are selected ion chromatograms [each consisting of *m/z* 466 (cholylglycine) and *m/z* 408 (cholanamide)]. Chromatogram A is for the reaction products in the absence of added PAM and contains only *m/z* 466 (cholylglycine). Chromatogram B is for the reaction products with PAM and contains only *m/z* 408 (cholanamide, the major peak). The minor peak in this chromatogram is the ammonia adduct of a detergent (*m/z* 391).
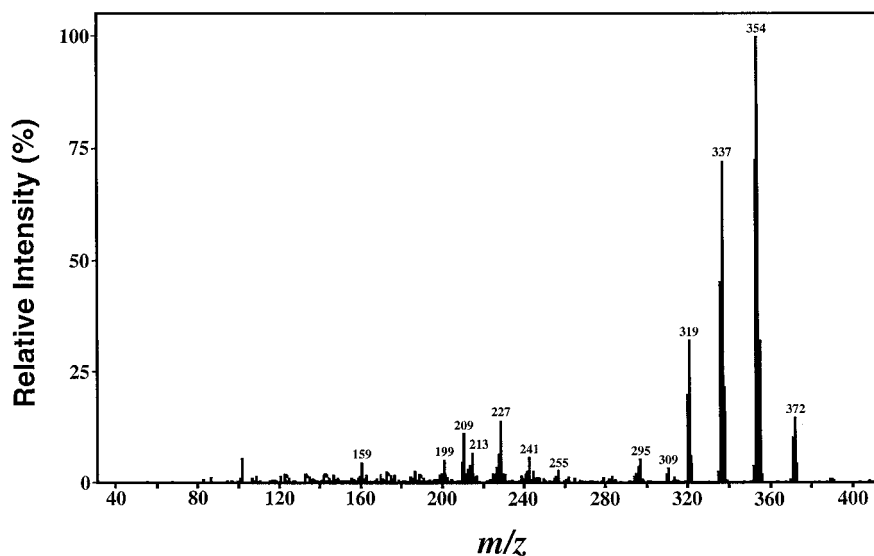
FIG. 2. Tandem mass spectrometry of the cholanamide m/z 408 peak in Fig. 1. The reaction mixture following incubation of cholylglycine with PAM was analyzed by reversed-phase HPLC and ESI-MS as described in Fig. 1. The IonSpray needle voltage was 5500 V and the orifice potential +75 V. Ions (m/z 408) were selected in the first quadrupole filter and then allowed to collide with argon–10% nitrogen gas. Fragment ions were analyzed in the third quadrupole to obtain the daughter ion mass spectrum.

uncoupling of O_2 reduction from substrate oxidation. Oxidative cleavage of the glycyl moiety of any bile acid glycine conjugates, as catalyzed by bifunctional PAM, would lead to the production of glyoxylate (7, 13, 30). Glyoxylate is formed upon the incubation of four different bile acid glycine conjugates with PAM (Table II), indicative of C_α–N bond scission in the glycyl moiety. Further analysis of the reaction mixtures by LC-MS shows that PAM converts the bile acid glycine conjugates to the corresponding bile acid amides (Table III).

The PAM-mediated amidation of glycine-extended peptides (24, 36), N-acylglycines (13), and N-arylglycines (42) proceeds through an α-hydroxyglycine, carbinolamide intermediate. The carbinolamide is subsequently dealkylated to the amide and glyoxylate. The individual catalytic domains of bifunctional PAM (or monofunctional PHM and PAL) catalyze the two steps of the amidation reaction. The addition of PAM to cholylglycine results in the consumption of O_2 at a rate that is approximately fourfold higher than the rate of

TABLE III

m/z Values for the Products of the Reaction between PAM and the Bile Acid Glycine
Conjugates as Determined by LC-ESI-MS

Glycine conjugate (substrate)	(+/−)	Unreacted (substrate)	Bile acid amide[a] (product)	Carbinolamide (intermediate)
Cholylglycine	+ve	466 [M + H]$^+$	408 [M + H]$^+$	Not observed
	−ve	464 [M − H]$^-$	466 [M − H + 60]$^-$	480 [M − H]$^-$
Deoxycholylglycine	+ve	450 [M + H]$^+$	392 [M + H]$^+$	Not observed
	−ve	448 [M − H]$^-$	436 [M − H + 46]$^-$	464 [M − H]$^-$
Chenodexoycholylglycine	+ve	450 [M + H]$^+$	392 [M + H]$^+$	Not observed
	−ve	448 [M − H]$^-$	436 [M − H + 46]$^-$	464 [M − H]$^-$
3-Sulfolithocholylglycine	+ve	Not observed	392 [M + H]$^+$	Not observed
	−ve	512 [M − H]$^-$	454 [M − H]$^-$	Not observed

Note. Reactions were initiated by the addition of 180 μg of PAM to 3.5 ml of 20 mM Mes/NaOH pH 6.0, 0.001% (v/v) Triton X-100, 1.0 mM sodium ascorbate, 1.0 μM Cu(NO$_3$)$_2$, 10 μg/ml bovine catalase, 200 μM bile acid glycine conjugate, and 0 or 30 μM N-Ac-Phe-pyruvate. The PAL-specific inhibitor, N-Ac-Phe-pyruvate, was included in the duplicate samples to facilitate the accumulation of the carbinolamide intermediate. The samples were quick frozen in liquid N$_2$ to terminate the reaction after a 20-min incubation at 37°C.

[a] The negative ion adducts depended on the composition of the HPLC solvent. For cholanamide, acetic acid (0.1%, v/v) was included in the solvent, whereas formic acid (0.1%, v/v) was used for the other bile acid amides.
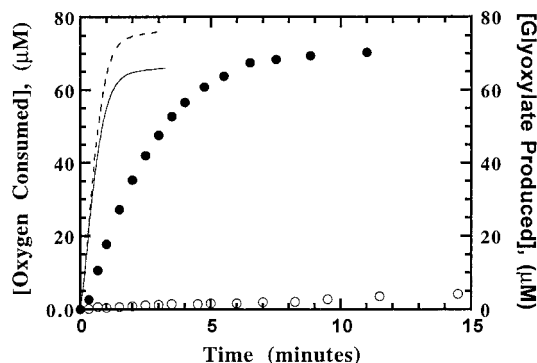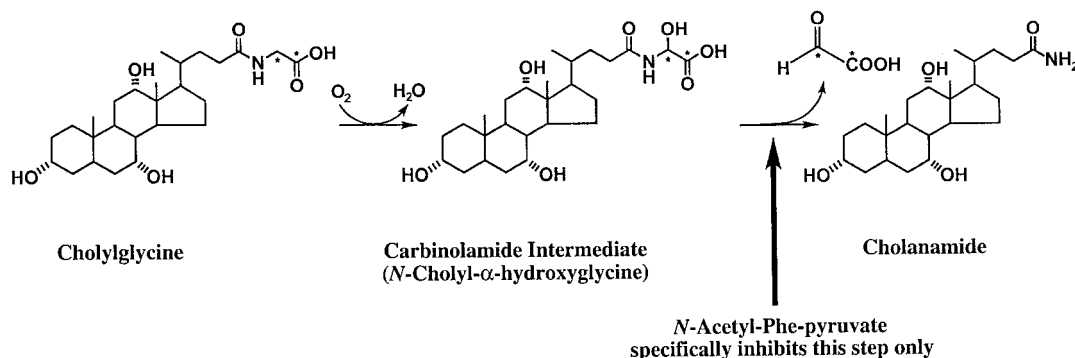
FIG. 3. The PAM-catalyzed consumption of O_2 (—) and the production of glyoxylate (●) from cholylglycine. Reactions at 37°C were initiated by the addition of PAM (74 μg) to 4.0 ml of 100 mM Mes/NaOH, pH 6.0, 30 mM NaCl, 1.0% (v/v) ethanol, 0.001% (v/v) Triton X-100, 10 μg/ml catalase, 1.0 μM Cu(NO$_3$)$_2$, 5.0 mM sodium ascorbate, and 75 μM cholylglycine. Progress curves for the consumption of O_2 (– – –) and the production of glyoxylate (○) from 75 μM cholylglycine and 22.5 μM N-Ac-Phe-pyruvate are also included. In one sample, O_2 consumption was measured using an O_2 electrode. In a matched second sample, aliquots were removed at the indicated time and added to a vial containing one-fifth volume of 6% (v/v) trifluoroacetic acid to quench the reaction. The concentration of glyoxylate in each quenched sample was determined spectrophotometrically (29, 30).

glyoxylate production (Fig. 3). The best explanation for this result is that an oxidized intermediate must first form from cholylglycine before the production of cholanamide and glyoxylate. By analogy to the earlier studies, the intermediate is likely to be N-cholyl-α-hydroxyglycine.

The hydroxylation/dealkylation of [*glycyl*-1,2-^{13}C$_2$]-cholylglycine was followed by ^{1}H–^{13}C HMQC NMR to identify the oxidized intermediate as N-cholyl-α-hydroxyglycine. Incubation of [*glycyl*-1,2-^{13}C$_2$]cholylglycine with PAM in the presence of a PAL-specific inhibitor results in the accumulation of a species with a ^{13}C chemical shift consistent with N-cholyl-α-hydroxyglycine (Fig. 4).

LC-MS of a similar reaction done using unlabeled cholylglycine is also consistent with the formation of N-cholyl-α-hydroxyglycine (Fig. 5 and Table III). The PAM-catalyzed amidation of the cholylglycine conjugates is, thus, completely analogous to the glycine-extended peptide and N-acylglycine reactions. The initial formation N-cholyl-α-hydroxyglycine is followed by dealkylation to cholanamide and glyoxylate (Scheme I).

The biosynthesis of bile acid amides. Bile acid-CoA: amino acid N-acyltransferase (BAT, EC 2.3.1.65) catalyzes the transfer of the bile acid moiety from bile acid-CoA to either glycine (H$_2$N–CH$_2$–COOH) and taurine (H$_2$N–CH$_2$–CH$_2$–SO$_3$H) to form the respective bile acid amidate. The sequential actions of BAT and PAM would convert the bile acid-CoA thioesters and glycine to the respective bile acid amides and glyoxylate (Scheme II).

Tissue distribution studies indicate that BAT is found only in the liver and kidney of mammals (43). The tissue distribution of mammalian PAM is widespread, with the highest concentrations being found in the hypothalamus, the pituitary, and the atria of the heart (17, 18, 23). Detectable levels of PAM are also found in the plasma (17, 18), the cerebrospinal fluid (44, 45), and throughout the central nervous system (17, 46–48). The liver and the kidney are virtually devoid of PAM (17–19). As a consequence, the biosynthesis of the bile acid amides is not likely to occur in the liver and the kidney. Instead, we propose that the bile acid glycine conjugates are first made in the liver and are then transported to tissue(s) containing PAM for subsequent amidation.

Two attractive sites for the PAM-catalyzed amidation of the bile acid glycine conjugates are the blood and the choroid plexus. The bile acid glycine conjugates are known to accumulate in both the blood (in cholestatic liver disease) (21, 22) and in the choroid plexus (49) and PAM has been identified in both (17, 18, 48).
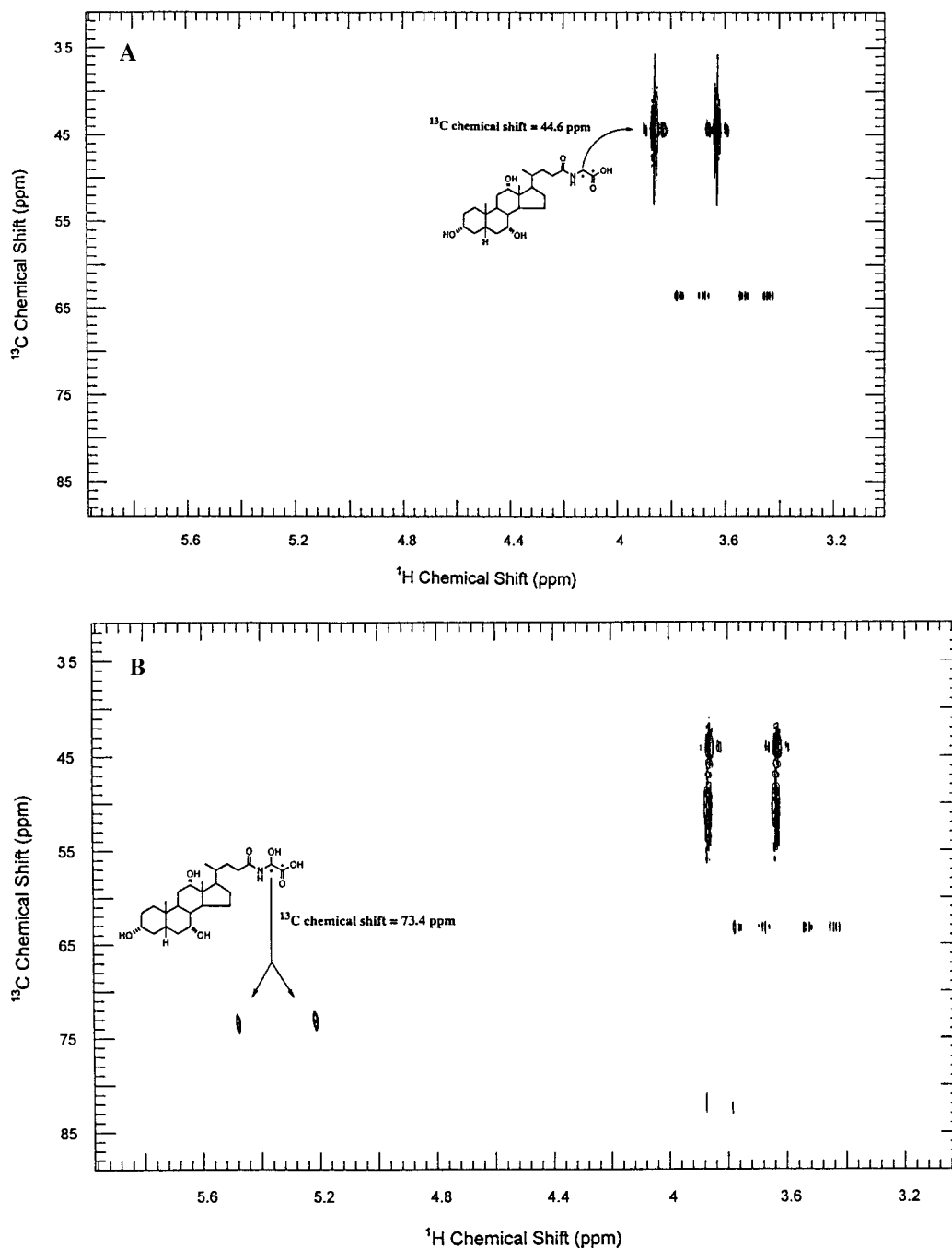

SCHEME I. The amidation of cholylglycine by bifunctional PAM. The positions indicated with the stars (★) are ^{13}C-labeled in [*glycyl*-1,2-^{13}C$_2$]cholylglycine.

FIG. 4. ^{1}H–^{13}C HMQC spectra of [*glycyl*-1,2-^{13}C$_2$]cholylglycine (A) and of enzymatically generated [α-*hydroxyglycyl*-1,2-^{13}C$_2$]-*N*-cholyl-α-hydroxyglycine (B). Solutions (in 100% D$_2$O) containing 10 mM Mes/LiOD, pD 5.6, 4.0 mM NaCl, 10 μg/ml catalase, 1.0 μM Cu(NO$_3$)$_2$, 4.0 mM sodium ascorbate, 3.0 mM [*glycyl*-1,2-^{13}C$_2$]cholylglycine, 100 μM *N*-Ac-Phe-pyruvate, and either 0 (A) or 150 μg/ml PAM were incubated at 37°C for 3 h. PAM and catalase were removed prior to NMR analysis from both solutions using a Centricon-30 diafilter (Amicon). The NMR spectra were acquired at 600 MHz at 27°C and referenced to acetone as an external standard. Stock solutions of Mes, NaCl, sodium ascorbate, and Cu(NO$_3$)$_2$ were prepared in D$_2$O. Peaks at ca. 63 and 83 ppm on the carbon axis are due to buffer components.

Another possibility would be the transport of the bile acid glycine conjugates into the cerebrospinal fluid or the central nervous system and then their conversion

to the amides by the enzyme identified in these tissues. Organic anion transporters have been identified (50–52) that may enable bile acid glycine conjugates to
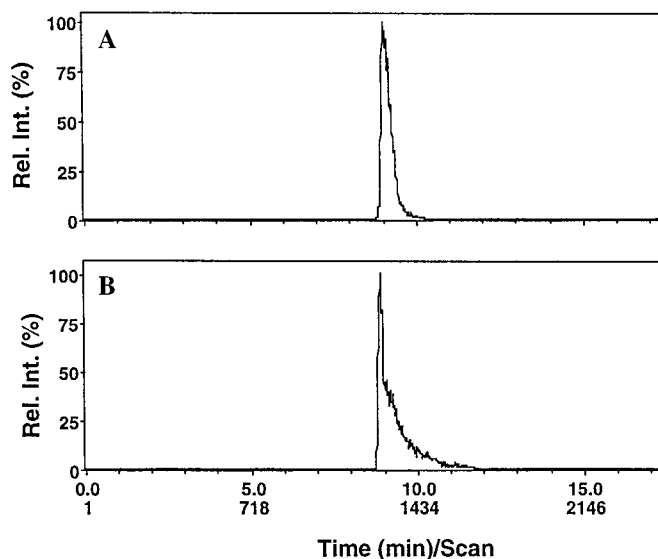
FIG. 5. LC-ESI-MS selected ion chromatogram of the reaction of cholylglycine with PAM in the presence of *N*-Ac-Phe-pyruvate. Reactions with cholylglycine were done as described in Fig. 1 except that 30 μM *N*-Ac-Phe-pyruvate was included in the incubation mixture. Aliquots (5 μl) of the incubation mixture were analyzed by LC-ESI-MS as described in Fig. 1. Mass spectra were recorded over a *m*/*z* range of 300–450 in the negative ion mode with the IonSpray voltage set at -7000 V. (A) Selected ion chromatogram for *m*/*z* 466, the peak being that of the acetate adduct of the $[M - H]^-$ ion of cholanamide. (B) Selected ion chromatogram for *m*/*z* 480, the peak being that of the $[M - H]^-$ ion of *N*-cholyl-α-hydroxyglycine.

these nonpeptide PAM substrates may also inhibit the normal production of the α-amidated neuropeptide hormones. Decreased production of neuropeptides may be at least partially responsible for the encephalopathy associated with liver disease (54, 55).
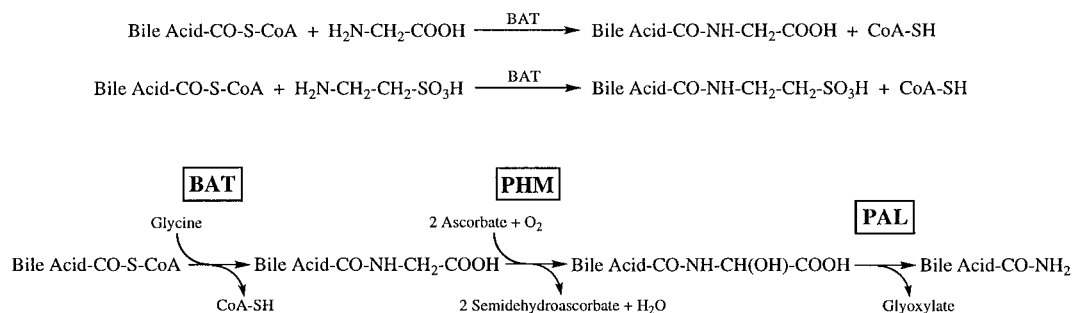
In conclusion, we have shown that bifunctional peptidylglycine α-amidating monooxygenase catalyzes the two-step conversion of the bile acid glycine conjugates to the bile acid amides and glyoxylate via a carbinolamide intermediate. The bile acid amides have never been isolated from a biological system (for a review of bile acid metabolism, see Ref. 56) but, if so, may represent a previously unrecognized class of cell signaling molecules.

cross the blood–brain barrier. However, receptor-mediated transport may not be required for the bile acid glycine conjugates to cross the blood–brain barrier. These molecules most likely have the dual criteria of sufficient lipid solubility and low molecular weight ($<$500 Da) for the unassisted, lipid-mediated movement from the blood into the brain (53).

Liver dysfunction often results in elevated concentrations of the bile acid glycine conjugates in the blood (21, 22). If bile acid glycine conjugates are able to cross the blood–brain barrier, increased concentration of

REFERENCES

1. Merkler, D. J. (1994) *Enzyme Microb. Technol.* **16,** 450–456.
2. Konopinska, D., Rosinski, G., and Sobótka, W. (1992) *Int. J. Pept. Protein Res.* **39,** 1–11.
3. Grimmelikhuijzen, C. J. P., Leviev, I., and Carstensen, K. (1996) *Int. Rev. Cytol.* **167,** 37–89.
4. Cravatt, B. F., Prospero-Garcia, O., Siuzdak, G., Gilula, N. B., Henriksen, S. J., Boger, D. L., and Lerner, R. A. (1995) *Science* **268,** 1506–1509.
5. Wakamatsu, K., Masaki, T., Itoh, F., Kondo, K., and Sudo, K. (1990) *Biochem. Biophys. Res. Commun.* **168,** 423–429.
6. Boger, D. L., Henrikson, S. J., and Cravatt, B. F. (1998) *Curr. Pharm. Des.* **4,** 203–214.
7. Bradbury, A. F., Finnie, M. D. A., and Smyth, D. G. (1982) *Nature* **298,** 686–688.
8. Eipper, B. A., Mains, R. E., and Glembotski, C. C. (1983) *Proc. Natl. Acad. Sci. USA* **80,** 5144–5148.
9. Mains, R. E., Park, L. P., and Eipper, B. A. (1986) *J. Biol. Chem.* **261,** 11938–11941.
10. Merkler, D. J., Merkler, K. A., Stern, W., and Fleming, F. F. (1996) *Arch. Biochem. Biophys.* **330,** 430–434.
11. Klinman, J. P. (1996) *Chem. Rev.* **96,** 2541–2561.

SCHEME II. The reactions catalyzed by BAT and the sequential actions of BAT and PAM producing the bile acid amides.

12. Kulathila, R., Merkler, K. A., and Merkler, D. J. (1999) *Nat. Prod. Rep.* **16,** 145–154.

13. Wilcox, B. J., Ritenour-Rodgers, K. J., Asser, A. S., Baumgart, L. E., Baumgart, M. A., Boger, D. L., DeBlassio, J. L., deLong, M. A., Glufke, U., Henz, M. E., King, L., III, Merkler, K. A., Patterson, J. E., Robleski, J. J., Vederas, J. C., and Merkler, D. J. (1999) *Biochemistry* **38,** 3235–3245.

14. Schachter, D., and Taggart, J. V. (1954) *J. Biol. Chem.* **208,** 263–275.

15. Bartlett, K., and Gompertz, D. (1974) *Biochem. Med.* **10,** 15–23.

16. Asaoka, K. (1991) *Int. J. Biochem.* **23,** 429–434.

17. Wand, G. S., Ney, R. L., Baylin, S., Eipper, B. A., and Mains, R. E. (1985) *Metabolism* **34,** 1044–1052.

18. Eipper, B. A., Myers, A. C., and Mains, R. E. (1985) *Endocrinology* **116,** 2497–2504.

19. Dickinson, C. J., Takeuchi, T., Guo, Y.-J., Stadler, B. T., and Yamada, T. (1993) *Am. J. Physiol.* **264,** G553–G560.

20. Falany, C. N., Johnson, M. R., Barnes, S., and Diasio, R. B. (1994) *J. Biol. Chem.* **269,** 19375–19379.

21. Kuipers, F., Bijleveld, C. M. A., Kneepkens, C. M. F., van Zanten, A., Fernandes, J., and Vonk, R. J. (1985) *Scand. J. Gastroenterol.* **20,** 1255–1261.

22. Qiu, B. S., Cho, C. H., and Ogle, C. W. (1992) *Horm. Metab. Res.* **24,** 443–445.

23. Eipper, B. A., May, V., and Braas, K. M. (1988) *J. Biol. Chem.* **263,** 8371–8379.

24. Mounier, C. E., Shi, J., Sirimanne, S. R., Chen, B.-H., Moore, A. B., Gill-Woznichak, M. M., Ping, D., and May, S. W. (1997) *J. Biol. Chem.* **272,** 5016–5023.

25. Bertelsen, A. H., Beaudry, G. A., Galella, E. A., Jones, B. N., Ray, M. L., and Mehta, N. M. (1990) *Arch. Biochem. Biophys.* **279,** 87–96.

26. Matthews, D. E., Piparo, K. E., Burkett, V. H., and Pray, C. C. (1994) *in* Animal Cell Technology: Products of Today, Prospects for Tomorrow (Spier, R. E., Griffiths, J. B., and Bethold, W., Eds.), pp. 315–319, Butterworth-Heinemann Ltd., Oxford, UK.

27. Miller, D. A., Sayad, K. U., Kulathila, R., Beaudry, G. A., Merkler, D. J., and Bertelsen, A. H. (1992) *Arch. Biochem. Biophys.* **298,** 380–388.

28. Jones, B. N., Tamburini, P. P., Consalvo, A. P., Young, S. D., Lovato, S. J., Gilligan, J. P., Jeng, A. Y., and Wennogle, L. P. (1988) *Anal. Biochem.* **168,** 272–279.

29. Christman, A. A., Foster, P. W., and Esterer, M. B. (1944) *J. Biol. Chem.* **155,** 161–171.

30. Katopodis, A. G., and May, S. W. (1990) *Biochemistry* **29,** 4541–4548.

31. Cleland, W. W. (1979) *Methods Enzymol.* **63,** 103–138.

32. Tamburini, P. P., Young, S. D., Jones, B. N., Palmesino, R. A., and Consalvo, A. P. (1990) *Int. J. Pept. Protein Res.* **35,** 153–156.

33. Landymore-Lim, A. E. N., Bradbury, A. F., and Smyth, D. G. (1983) *Biochem. Biophys. Res. Commun.* **117,** 289–293.

34. Merkler, D. J., Kulathila, R., Consalvo, A. P., Young, S. D., and Ash, D. E. (1992) *Biochemistry* **31,** 7282–7288.

35. Young, S. D., and Tamburini, P. P. (1989) *J. Am. Chem. Soc.* **111,** 1933–1934.

36. Katopodis, A. G., Ping, D., and May, S. W. (1990) *Biochemistry* **29,** 6115–6120.

37. Merkler, D. J., and Young, S. D. (1991) *Arch. Biochem. Biophys.* **289,** 192–196.

38. Eipper, B. A., Stoffers, D. A., and Mains, R. E. (1992) *Annu. Rev. Neurosci.* **15,** 57–85.

39. Pretsch, E., Seibl, J., and Simon, W. (1989) Tables of Spectral Data for Structure Determination of Organic Compounds, 2nd ed., Springer-Verlag, Berlin.

40. Erion, M. D., Tan, J., Wong, M., and Jeng, A. Y. (1994) *J. Med. Chem.* **37,** 4430–4437.

41. Prigge, S. T., Kolhekar, A. S., Eipper, B. A., Mains, R. E., and Amzel, L. M. (1997) *Science* **278,** 1300–1305.

42. Kawahara, T., Suzuki, K., Iwasaki, Y., Shimoi, H., Akita, M., Moro-oka, Y., and Nishikawa, Y. (1992) *J. Chem. Soc. Chem. Commun.* 625–626.

43. Falany, C. N., Fortinberry, H., Leiter, E. H., and Barnes, S. (1997) *J. Lipid Res.* **38,** 1139–1148.

44. Wand, G. S., May, C., May, V., Whitehouse, P. J., Rapoport, S. I., and Eipper, B. A. (1987) *Neurology* **37,** 1057–1061.

45. Tsukamoto, T., Noguchi, M., Kayama, H., Watanabe, T., Asoh, T., and Yamamoto, T. (1995) *Intern. Med.* **34,** 229–232.

46. Graham, L., and Gallop, P. M. (1989) *Brain Res.* **491,** 371–373.

47. Rhodes, C. H., Xu, R.-Y., and Angeletti, R. H. (1990) *J. Histochem. Cytochem.* **38,** 1301–1311.

48. Gee, P., Rhodes, C. H., Fricker, L. D., and Angeletti, R. H. (1993) *Brain Res.* **617,** 238–248.

49. Bárány, E. H. (1975) *Acta Physiol. Scand.* **93,** 250–268.

50. Smith, Q. R., Momma, S., Aoyagi, M., and Rapoport, S. I. (1987) *J. Neurochem.* **49,** 1651–1658.

51. Angeletti, R. H., Bergwerk, A. J., Novikoff, P. M., and Wolkoff, A. W. (1998) *Am. J. Physiol.* **275,** C882–C887.

52. Abe, T., Kakyo, M., Sakagami, H., Tokui, T., Nishio, T., Tanemoto, M., Nomura, H., Hebert, S. C., Matsuno, S., Kondo, H., and Yawo, H. (1998) *J. Biol. Chem.* **273,** 22395–22401.

53. Pardridge, W. M. (1997) *J. Cereb. Blood Flow Metab.* **17,** 713–731.

54. Collis, I., and Lloyd, G. (1992) *Br. J. Psychiatry* **161,** 12–22.

55. Ananth, J., Swartz, R., Burgoyne, K., and Gadasally, R. (1994) *Psychother. Psychosom.* **62,** 146–159.

56. Barnes, S. (1991) *in* Oxford Textbook of Clinical Hepatology (McIntyre, N., Benhamou, J.-P., Bircher, J., Rizzetto, M., and Rodes, J., Eds.), Vol. 1, pp. 115–129, Oxford Univ. Press, Oxford.